Journal of Food Engineering 94 (2009) 344–349

Contents lists available at ScienceDirect

Journal of Food Engineering

journal homepage: www.elsevier.com/locate/jfoodeng

Convection and radiation combined surface heat transfer coefficient in baking ovens

Melike Sakin *, Figen Kaymak-Ertekin, Coskan Ilicali [1]

Ege University, Faculty of Engineering, Department of Food Engineering, 35100 Bornova, Izmir, Turkey

ARTICLE INFO

Article history:
Received 11 November 2008
Received in revised form 24 March 2009
Accepted 31 March 2009
Available online 5 April 2009

Keywords:
Heat transfer coefficient
Baking
Convective oven

ABSTRACT

The combined surface heat transfer coefficient is a determining parameter of convective baking process time and efficiency, as well as the resulting food product quality. By this study, the combined surface heat transfer coefficient term was determined at the convective oven temperature range of 70–220 °C, with fan (turbo) and without fan (static oven) applications. The methods of "Lumped Capacity" and "Time–Temperature Matching" were used. Both methods utilize the time–temperature data at a fixed position of a definite material, during unsteady state heating up period inside the convective oven. The increase in oven temperature and the fan application in the oven derived higher calculated values of surface heat transfer coefficients. Good agreement was observed between both methods and the literature values. The given methods are applicable to other oven types and heating modes.

1. Introduction

As one of the oldest and most popular food processing techniques, baking has been under investigation by many research teams to improve the energy efficiency of the process as well as the food product physical and sensorial quality (Savoye et al., 1992; Sablani et al., 1998; Lostie et al., 2002; Baik and Marcotte, 2002; Sakin, 2005; Sakin et al., 2007a,b). In a baking oven, the hot air flows over the baking material either by natural convection or forced by a fan, the convection heat transfer from the air, the radiation heat transfer from the oven heating surfaces, and the conduction heat transfer across contact area between product and metal surface. The moisture in the food material simultaneously diffuses toward the surfaces, then, it transfers from the surface by convection, and the product looses moisture with continuous movement of the oven ambient air. These are the simultaneous momentum, heat and moisture transfer mechanisms within a baking product (Tong and Lund, 1990; Özilgen and Heil, 1994; Zanoni et al., 1993, 1994; Thorvaldsson and Janestad, 1999) and between the product and its environment (Standing, 1974; Carvalho and Martins, 1993; Broyart and Trystram, 2002), which, theoretically, are well known.

The determination and prediction of transport properties (the convection, radiation or combined surface heat transfer coefficients, thermal diffusivity and thermal conductivity of the material, the surface convective moisture transfer coefficient, moisture diffusivity) during baking are essential in baking process mathematical modeling (Singh et al., 1984; Sato et al., 1987; Zanoni et al., 1994; Pan et al., 2000; Nitin and Karwe, 2001; Pan and Singh, 2002; Carson et al., 2006; Demirkol et al., 2006; Sakin and Turkkan, 2006; Sakin et al., 2007a). Among the heat transport parameters, the surface heat transfer coefficient term, which expresses the combined effects of oven heating mode (top and/or up heaters or grill on), air and heating surface temperatures, air velocity and physical properties of air, is one of the determining parameters of the baking process time and efficiency together with the resulting product quality. The term is usually reported as a combination of thermal convection and radiation heat transfer coefficients. In determining the surface heat transfer coefficient, h (W/m^{2}K), one approach is the use of Nusselt correlations for convective boundary conditions only, while another approach for combined surface heat transfer coefficient is the use of the lumped capacity method, where the use of it is based on the hypothesis that the temperature within the solid is spatially uniform and that Biot number must be check to ensure the validity of the method (Geankoplis, 2003). Also, through measurement of heat flux at the surface of the material by a heat flux sensor, the surface heat transfer coefficient term can be calculated. However, these sensors can also change the boundary layer and the surface conditions (Tszeng and Saraf, 2003).

By using aluminum disks instead of model food products, by the lumped capacity method, Nitin and Karwe (2001) found that the heat transfer correlations developed for discrete, cookie shaped objects under ARN (array of round nozzles) flow were similar to those developed for heat transfer to a flat plate. Erdoğdu et al. (2005) investigated the spatial variation of h-value over a disk shaped

Abbreviations: LC, lumped capacity; TTM, time–temperature matching.

* Corresponding author. Tel.: +90 232 3884000x3039; fax: +90 232 3427592.
E-mail address: melike.sakin@ege.edu.tr (M. Sakin).
[1] Present address: Kyrgyzstan-Turkey Manas University, Faculty of Engineering, Department of Food Engineering, 720042 Bishkek, Kyrgyzstan.

0260-8774/$ - see front matter © 2009 Elsevier Ltd. All rights reserved.
doi:10.1016/j.jfoodeng.2009.03.027

Nomenclature

A	area (m^2)
Bi	Biot number for heat transfer
c_p	specific heat (J/kgK)
$D(i,j)$, $d(i,j)$	elements of the right-hand side vector
f', f''	a variable
g	a variable
gamma	dimensionless time
H	height (m) or the position at the full height of the Al cylinder
h	surface heat transfer coefficient (W/m^2 K)
i	the ith node in the radial direction
j	the jth node in the upward direction
k	thermal conductivity (W/mK)
L	length (m)
ℓ	a variable
M, m	number of intervals in z direction
MP1	$M+1$, the top surface layer
N, n	number of intervals in r direction
NP1	$N+1$, the radial axis
p, p'	variable defined in the related equation, or probability
r, R	radial direction, radius
s	a variable
T	temperature (°C)
$T_{i,j}$, $T'_{i,j}$, $T^*_{i,j}$	temperature at (i,j)th position (°C)
T_r; T_s	oven wall; product surface temperature (K)
t	time (s)
v	velocity (m/s)
V	volume (m^3)
W	width (m)
y, yy	a variable
z	upward direction

Subscripts

a	ambient
c	convective
ini	initial
k	combined
r	radiative
r, z	the r and z directions
s	surface
∞	baking oven environment

Greek symbols

α	thermal diffusivity (m^2/s)
Δr, Δz	spatial increments in r and z directions
Δt	time step (s)
ε	emissivity
φ	wire diameter (m)
v	a variable
ρ	density (kg/m^3)
σ	Stefan–Boltzman coefficient ($W/m^2/K^4$)

copper surface during cooling under impinged air conditions, where they used the time temperature data for copper disk. The h-values were determined applying the lumped system analysis. The transient time–temperature change was predicted by a numerical model, which was a three-dimensional explicit finite difference mathematical model, developed and validated, where the agreement between the model predictions and the experimental data was stated as excellent.

Another approach in the determination of surface heat transfer coefficient is to use an iterative technique, with an inverse heat transfer analysis; which is referred in this work as "time–temperature matching method". In this technique, there exist a model system of a well-defined geometry and known thermophysical properties. The temperature history at a fixed position of the model system is measured and the heat transfer coefficient is estimated iteratively, using either analytical or numerical solutions of heat transfer (Anderson and Singh, 2006). Singh (1982) used this method for thermal diffusivity determination.

In their study, Verboven et al. (2003) calculated the magnitude and distribution of the surface heat transfer coefficient on the food surface under various conditions, by 3-D modeling of the cylindirical food placed in the center of the airspace in the oven. The governing Navier–Stokes and energy equations were solved numerically using a commercial CFD code for laminar flow, the average surface heat transfer coefficient chosen as the variable to follow convergence, by the Richardson extrapolation method.

The objective of this study was to determine the surface heat transfer coefficient as a combined term, implying both the convection and radiation affects, during convective oven baking, at the oven temperature range of 70–220 °C, with fan and without fan applications. The methods of "Lumped Capacity" and "Time–Temperature Matching" were used for the calculation of surface heat transfer coefficient and the results obtained by both methods were compared with one another.

2. Materials and methods

2.1. Materials

Temperature controlled (±1 °C), domestic type electrical convective baking oven (Teba High-01 Inox), which was 0.39 × 0.44 × 0.35 ($L \times W \times H$) in dimensions (m), was used at the experimental stage. It has "with fan" and "without fan" conditions that can be alternatively used. The fan provided an air velocity of 0.56 m/s, measured inside the oven cavity by an anemometer (Airflow anemometer, LCA 6000, UK). The oven was preheated before the heating experiments to eliminate the deviations in wall temperatures and to provide constant radiant heat.

The Aluminum cylinder having 6 cm diameter and 10.1 cm height was used for the determination of heat transfer coefficient. It was placed on the metal wires within the oven cavity. The cylinder has two holes that allowed temperature measurement at the radial axis and half radial positions at the height corresponding to the half length of the cylinder. The cylindrical surface was heavily oxidized Aluminum surface, the emissivity (ε) being 0.33 (Geankoplis, 2003).

J type thermocouples (wire size, Ø: 1 mm; accuracy: 1–1.5 °C), that were calibrated in water and ice baths against a standard glass mercury thermometer, were used for temperature measurements at the radial axis of the Aluminum cylinder and of the oven environment. Thermocouples were held in position, at the geometric centre of the cylinder, by heat resistant plasters (3 M, USA). The multi-channel data-logger (HANNA Instruments, HI 98804, Portugal) having an accuracy of ±0.5 °C, excluding the probe error, was used for logging the measured temperature profile to the computer. The temperature at the oven wall surfaces (bottom, top, side) was measured by an infrared-non contact thermometer (Testo, 825-T2) having an accuracy of ±2 °C. The temperature measurements were done as three parallels. The wall surface (bottom, top,

side) temperatures were measured at many position of that surface and the average value was taken.

2.2. Methods

The surface heat transfer coefficient is a significant parameter in the experimental and mathematical analysis of the baking process. The parameter, considered here, combined the effects of the simultaneous convection and radiation heat transfer, to the object being heated inside the oven. The combined surface heat transfer coefficient, h_k (W/m^2 K) is the sum of the convective surface heat transfer coefficient, h_c (W/m^2 K) plus the radiative surface heat transfer coefficient, h_r (W/m^{2}K), as given in Eq. (1)

$$h_k = h_c + h_r \tag{1}$$

In the determination of the combined surface heat transfer coefficient, "the lumped capacity (LC)" and "the time–temperature matching (TTM)" methods were used. Both methods utilized the experimental time–temperature data recorded at the geometric centre of the defined material (the Aluminum cylinder), during the unsteady-state heating up period inside the convective oven, at 70, 100, 130, 160, 190 and 220 °C oven temperatures, under conditions of with and without fan.

The dimensions (m), density (ρ, kg/m^3), the thermal conductivity (k, W/mK), the specific heat (c_p, J/kgK), thermal diffusivity (α, m^2/s), the surface emissivity of Aluminum are all known and assumed to be constant.

2.2.1. Lumped capacity method

The principle of the "Lumped capacity method" is simply the assumption of a uniform temperature distribution within the material, at any time of an unsteady-state heating process. Negligible internal resistance assumption will be a sound assumption in metals due to their high thermal conductivities ($Bi < 0.1$), together with a proper magnitude of the intensity of heat transfer coefficient (Incropera and Dewitt, 1996).

The total heat transferred to the surface of the material, both by convection and radiation mechanisms, increases the internal energy of the material. The conduction heat transfer across the contact area between aluminum cylinder and metal wires, supporting the cylinder in the oven cavity, was assumed negligible, since the contact area was very small compared to the total surface area of the cylinder.

Through integration of the partial derivative of the internal temperature with respect to time the following linear relationship (Eq. (2)) may be obtained.

$$-\ln\left(\frac{T_\infty - T(t)}{T_\infty - T_{ini}}\right) = \frac{h_k A_{surface}}{\rho c_P V} t \tag{2}$$

where, T_∞ is the oven temperature (°C), T_{ini} is the initial temperature of the material (°C), $A_{surface}$ is the surface area of the material (m^2), V is the volume (m^3), ρ (kg/m^3) and c_P (J/kgK) are the density and specific heat of the material, respectively, t is time (s). From the slope of the dimensionless temperature curve, the combined surface heat transfer coefficient, h_k was calculated, by the Eq. (2). The Biot number in the experimental system was checked so that the spatial variations of product temperature can be neglected, as assumed.

2.2.2. Time–temperature matching method

The time–temperature method depends on the numerical solution of the Fourier equation (Eq. (3)) in the cylindrical geometry by the implicit alternating direction finite difference technique (Carnahan et al., 1969).

$$\frac{\partial T}{\partial t} = \alpha \cdot \left[\frac{\partial^2 T}{\partial r^2} + \frac{1}{r}\cdot\frac{\partial T}{\partial r} + \frac{\partial^2 T}{\partial z^2}\right] \tag{3}$$

A uniform initial temperature distribution was assumed (Eq. (4)) at all positions of the material, i.e.:

$$t = 0, \quad T = T_{ini} \quad \text{at all } r \text{ and } z \tag{4}$$

Convective heat transfer boundary conditions were valid for top/bottom and side surfaces (Eq. (5)):

$$k \cdot \frac{\partial T}{\partial z} = h_k \cdot (T_a - T_{surface}) \tag{5}$$

The radial axis and the half thickness were the symmetry axis (Eq. (6)),

$$\left.\frac{\partial T}{\partial r}\right|_{r=0,z=z} = 0 \tag{6}$$

It was assumed that thermophysical properties of the material and combined heat transfer coefficient were constant. A grid system was formed, i *and* j being the radial and axial directions, respectively. $i = 1$ indicated the lateral surface, $i = np1(n+1)$ the radial axis; $j = 1$ the lower surface; $j = mp1(m+1)$ the top surface (Fig. 1).

For the solution of temperature profile at the half time step ($T^*_{i,j}$), the tridiagonal matrix system was written as below:

In Fig. 2:

$$g = \frac{\alpha \times \Delta t/2}{\Delta z^2}, \quad s = \frac{\alpha \times \Delta t/2}{\Delta r^2}$$
$$p = h_k 2\Delta z/k \cdot g, \quad p' = h_k 2\Delta r/k \cdot s$$
$$y = 1/(2\cdot(n+1-i)), \quad yy = 1/2n$$
$$\ell = 2\Delta z/k, \quad v = 2\Delta r/k,$$
$$f' = (h_k T_a)\cdot \ell \cdot g, \quad f'' = (h_k T_a) v \cdot s$$

By the solution of the matrix system by the Gauss elimination method, the temperature profile $T^*_{i,j}$ was obtained at the ith column at all rows, at the half time period. After repeating the calculation for all columns, the $T^*_{i,j}$ at the whole grid points were reached. The known vector, $D_{i,j}$, was defined as below

$$d_{1,1} = (1-2s)T_{1,1} + (2s)T_{2,1} + v\cdot h_k(T_a - T_{1,1})\cdot s\cdot(1+yy) + f'$$
$$d_{1,j} = (1-2s)T_{1,j} + (2s)T_{2,j} + v\cdot h_k(T_a - T_{1,j})\cdot s\cdot(1+yy)$$
$$d_{1,m+1} = (1-2s)T_{1,m+1} + (2s)T_{2,m+1} + v\cdot h_k(T_a - T_{1,m+1})\cdot s\cdot(1+yy) + f'$$

$$\left.\begin{aligned} d_{i,1} &= s(1+y)T_{i-1,1} + (1-2s)T_{i,1} + s(1-y)T_{i+1,1} + f' \\ d_{i,j} &= s(1+y)T_{i-1,j} + (1-2s)T_{i,j} + s(1-y)T_{i+1,j} \\ d_{i,m+1} &= s(1+y)T_{i-1,m+1} + (1-2s)T_{i,m+1} + s(1-y)T_{i+1,m+1} + f' \end{aligned}\right\} 2 \leqslant i \leqslant n$$

$$d_{n+1,1} = (1-4s)T_{n+1,1} + (4s)T_{n,1} + f'$$
$$d_{n+1,j} = (1-4s)T_{n+1,j} + (4s)T_{n,j}$$
$$d_{n+1,m+1} = (1-4s)T_{n+1,m+1} + (4s)T_{n,m+1} + f'$$

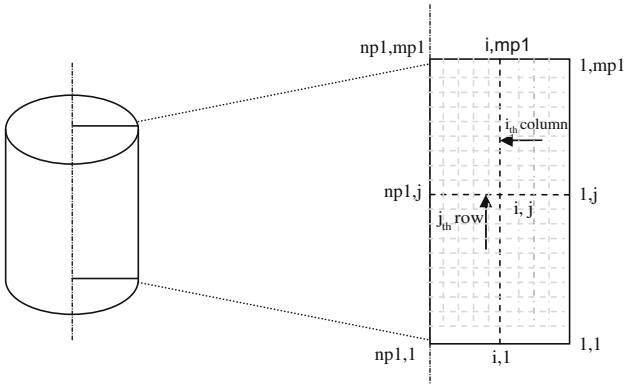

Fig. 1. The grid system in cylindrical geometry.

$$\begin{bmatrix} 1+2g+p & -2g & & & \\ \cdots\cdots & \cdots\cdots & \cdots\cdots & & \\ & -g & 1+2g & -g & \\ & & \cdots & \cdots & \\ & & & -2g & 1+2g+p \end{bmatrix} \begin{bmatrix} T^*_{i,1} \\ \cdots\cdots \\ T^*_{i,j} \\ \cdots \\ T^*_{i,m+1} \end{bmatrix} = \begin{bmatrix} d_{i,1} \\ \cdots\cdots \\ d_{i,j} \\ \cdots \\ d_{i,m+1} \end{bmatrix}$$

Fig. 2. Tridiagonal matrix system (at $t = t + \Delta t/2$).

At the second time step ($t + \Delta t$), the temperature profile, $T'_{i,j}$, was solved by the solution of the below formed tridiagonal matrix (Fig. 3). The half time step temperature profiles are the known vector, this time.

By the solution of the matrix system by the Gauss elimination method, the temperature profile $T'_{i,j}$ was obtained at the jth row at all columns, at the full time period. After repeating the calculation for all the rows, the $T'_{i,j}$ at the whole grid points were reached. The known vector, $D_{i,j}$, was defined as below

$$d_{1,1} = (1-2g)T^*_{1,1} + (2g)T^*_{1,2} + h_k(T_a - T^*_{1,1}) \cdot \ell \cdot g + f''(yy+1)$$
$$d_{i,1} = (1-2g)T^*_{i,1} + (2g)T^*_{i,2} + h_k(T_a - T^*_{i,1}) \cdot \ell \cdot g$$
$$d_{np1,1} = (1-2g)T^*_{np1,1} + (2g)T^*_{np1,2} + h_k(T_a - T^*_{np1,1}) \cdot \ell \cdot g$$

$$\left.\begin{aligned} d_{1,j} &= (1-2g)T^*_{1,j} + (g)T^*_{1,j-1} + (g)T^*_{1,j+1} + f''(yy+1) \\ d_{i,j} &= (1-2g)T^*_{i,j} + (g)T^*_{i,j-1} + (g)T^*_{i,j+1} \\ d_{np1,j} &= (g)T^*_{np1,j-1} + (1-2g)T^*_{np1,j} + (g)T^*_{np1,j+1} \end{aligned}\right\} 2 \leqslant j \leqslant m$$

$$d_{1,mp1} = (1-2g)T^*_{1,mp1} + (2g)T^*_{1,m} + \ell \cdot g \cdot h_k(T_a - T^*_{1,mp1}) + f''(yy+1)$$
$$d_{i,mp1} = (1-2g)T^*_{i,mp1} + (2g)T^*_{i,m} + \ell \cdot g \cdot h_k(T_a - T^*_{i,mp1})$$
$$d_{np1,mp1} = (2g)T^*_{np1,m} + (1-2g)T^*_{np1,mp1} + \ell \cdot g \cdot h_k(T_a - T^*_{np1,mp1})$$

The solution was computed by the computer program written in MS Visual Basic programming language. The program was executed by inputting the physical properties of the material (dimensions, thermal conductivity, thermal diffusivity, and initial temperature), the ambient or oven temperature, and the assumed initial combined surface heat transfer coefficient term. In other words, the heating curves of Al cylinder, during unsteady-state heating process inside the baking oven were simulated.

A simple trial and error solution on heat transfer coefficient, h_k, was proceeded by narrowing the range of possible values, until the matching of the experimental and numerically calculated centre temperatures, with an error range of ±0.1 °C.

The experimental time–temperature data recorded during the unsteady-state heating of the Al material was used as to provide input values at certain heating times, and to enable a comparison between the simulated and measured temperature profiles to verify the evaluated surface heat transfer coefficient term.

2.2.3. Radiative heat transfer coefficient

The radiation heat transfer coefficient was calculated by Stefan–Boltzmann equation (Eq. (7)) (Holman, 1992; Thorvaldsson and Janestad, 1999),

$$\begin{bmatrix} 1+2s+p'(1+yy) & -2s & & & \\ \cdots\cdots & \cdots\cdots & \cdots\cdots & & \\ & -s(y+1) & 1+2s & -s(-y+1) & \\ & & \cdots & \cdots & \\ & & & -4s & 1+4s \end{bmatrix} \begin{bmatrix} T'_{1,j} \\ \cdots\cdots \\ T'_{i,j} \\ \cdots \\ T'_{np1,j} \end{bmatrix} = \begin{bmatrix} d_{1,j} \\ \cdots\cdots \\ d_{i,j} \\ \cdots \\ d_{np1,j} \end{bmatrix}$$

Fig. 3. Tridiagonal matrix system (at $t = t + \Delta t$).

$$h_r = \varepsilon_s \cdot \sigma \cdot (T_r^2 + T_s^2) \cdot (T_r + T_s) \quad (7)$$

where T_s is the product surface temperature (K), T_r is the oven wall temperature (K), ε_s is the surface emissivity of the material = ε_{Al} (oxidised) = 0.33, σ is Stefan–Boltzman coefficient (5.676×10^{-8} W/m^2 K^4).

3. Data analysis

The numerical solutions were conducted by the computer program written at MS Visual Basic 6.0 programming language. The statistical analysis was paired sample t-test done by using SPSS version 13.0.

4. Results and discussion

4.1. Combined surface heat transfer coefficient

The combined surface heat transfer coefficient term was calculated by the methods of "Lumped capacity" and "time–temperature matching", with fan and without fan oven conditions, within the oven medium temperature range of 70–220 °C. The calculated results were illustrated in Fig. 4.

It was observed that for the "with fan" oven condition (forced convection), the combined surface heat transfer coefficient term was not significantly affected by the oven temperature ($p > 0.05$), by the t-test applied separately to the results of both methods. The numerical values were calculated as 28–34 W/m^2 K (standard error: 1.4) by the method of "Lumped Capacity", and 24–31 W/m^2 K (standard error: 2.0) by the method of "time–temperature matching". In case of with fan oven condition, although both methods gave results in similar trends (Fig. 4), the difference in results was observed as statistically important ($p < 0.05$), the mean paired difference being 2.6 W/m^2 K, where the "lumped capacity method" gave the higher results at all oven temperatures.

At the "without fan" oven condition (natural convection), the combined surface heat transfer coefficient term was observed to increase with an increase in oven temperature (Fig. 4). It was calculated that the value changed in between 11 and 20 W/m^2 K (standard error: 0.6) by the method of "Lumped Capacity", and 10–21 W/m^2 K (standard error: 1.0) by the method of "time–temperature matching". The difference between the results of both methods at each oven temperature was not important ($p > 0.05$), statistically.

The two methods are comparable to each other when $Bi < 0.1$, where the internal resistance can be neglected, like in the case of Al cylinder used in this study, where the two methods evidently gave the similar results. However, the importance of the "time–

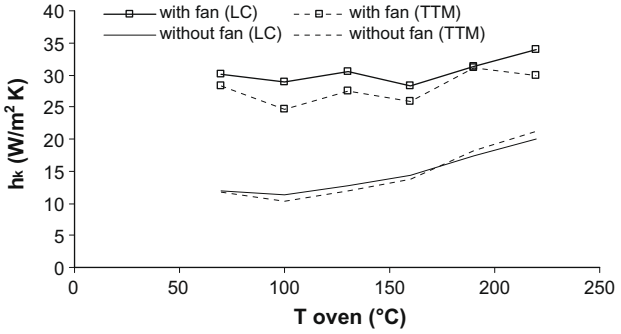

Fig. 4. The calculated combined surface heat transfer coefficients, "with fan" and "without fan" oven conditions (LC: Lumped Capacity Method, TTM: Time–Temperature Matching Method).

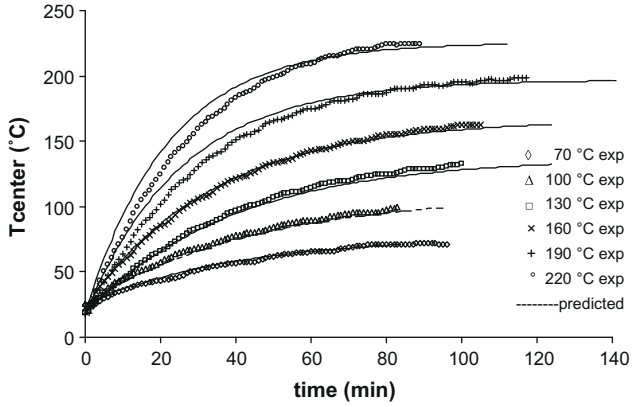

Fig. 5. Experimental and predicted (————) central temperature profiles, during heating at the "without fan" oven condition at different oven temperatures (◇: 70 °C, Δ: 100 °C, □: 130 °C, ×: 160 °C, +: 190 °C, ○: 220 °C).

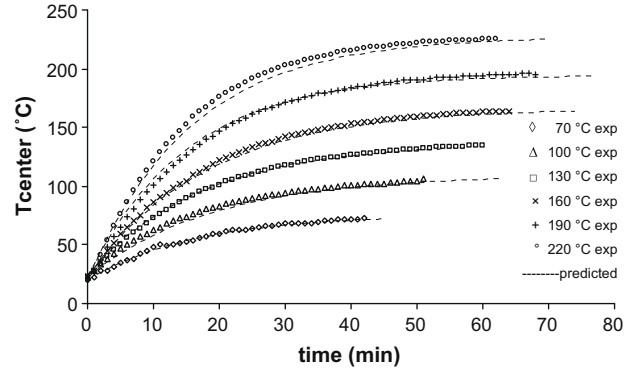

Fig. 6. Experimental and predicted (————) central temperature profiles, during heating at the "with fan" oven condition at different oven temperatures (◇: 70 °C, Δ: 100 °C, □: 130 °C, ×: 160 °C, +: 190 °C, ○: 220 °C).

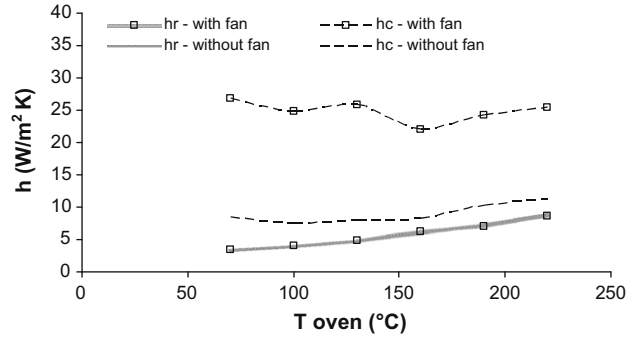

Fig. 7. Convective and radiative surface heat transfer coefficients, at "with fan" and "without fan" oven conditions.

temperature" matching method is seen by its use when the internal resistance is not neglectable. In other words, the time–temperature matching method can also be used without the pre-condition of $Bi < 0.1$, where the material is not metal but a Plexiglas, Teflon, or a food material.

4.2. Simulated heating curves

The heating curves of Al cylinder at the central position, during the unsteady-state heating process inside the baking oven were simulated. The calculated combined heat transfer coefficient term (by time–temperature matching method) was used as the input value to the numerical solution of the defined unsteady-state heating process. The numerical solution method was as given in Section 2.2.2. The good comparison achieved between the simulated and measured temperature profiles at both oven conditions verified the calculated surface heat transfer coefficient term (Figs. 5 and 6).

The calculated combined surface heat transfer coefficients from the experimental data were in accordance with the literature. In their study on the determination of combined surface heat transfer coefficient in forced convection oven, Carson et al. (2006) showed that this value changed in the range 15–40 W/m^2 K, as affected by the oven temperature. Sato et al. (1987) indicated that as the air velocity in the oven ranged from 0.2 to 1.5 m/s, the value of convective heat transfer coefficient increased from 5 to 20 W/m^2 K. Also, it was reported that an increase in the oven air temperature caused an increase in this coefficient. Nitin and Karwe (2001) showed that the heat transfer coefficient could be as high as 100 and 225 W/m^2 K in jet impingement oven when the air velocities were measured as 18–44 m/s.

4.3. The radiative and convective heat transfer coefficient

The calculated radiative (h_r) and the convective (h_c) surface heat transfer coefficients by Eqs. (7) and (1) were shown in Fig. 7 against the oven temperature, at the with fan and without fan oven conditions.

The convective heat transfer coefficient term showed higher values at the "with fan" oven condition, as expected because of the created forced convection effects by the fan. On the other hand, the radiative heat transfer coefficient was not affected by the oven fan condition, i.e. whether the fan was used or not. The lines of h_r for both condition overlapped each other. It was mainly affected by the increase in oven temperature which was a result of the higher heater surface temperatures. An increase in the ratio of the radiative heat transfer coefficient term (h_r) within the combined heat transfer coefficient (h_k) was observed with the increasing oven temperature. As the oven temperature increased from 70 °C up to 220 °C, this ratio increased from 11% to 25%, at the "with fan" oven condition; and from 29% to 44% at the "without fan" oven condition. In Table 1, the experimental average heater surface temperatures and the oven air temperatures were reported.

5. Conclusion

The combined surface heat transfer coefficient term during convective oven baking was determined, at the oven temperature range of 70–220 °C, with fan (turbo) and without fan (static air) applications. An increase in the surface heat transfer coefficient values was observed with the increase in oven temperature. Fan application resulted in higher heat transfer coefficients than no

Table 1
Oven wall surface average temperatures against oven medium temperatures.

Oven medium temperature (°C)		70	100	130	160	190	220
Oven wall surface average temperature, T_r (°C)	(with fan)	106.1	120.9	149.6	181.6	193.2	226.8
	(without fan)	110.6	123.6	147.0	186.7	217.9	243.9

fan application, as expected. The methods of "Lumped Capacity" and "Time–Temperature Matching" were used in the calculations. Good agreement was observed between both methods and the literature values. The given methods are applicable to other oven types and heating modes. The numerical "time–temperature matching method", that provided comparable results with the "Lumped Capasity" method, was proposed to be used even in the cases where the internal resistance can not be neglected.

Acknowledgements

The authors acknowledge the financial support to this project by Ege University, Council of Scientific Research Projects (Project No.: BAP 2002/Müh/014). And, equipment and material support of the companies of TEBA Günkol Solar Energy and Air Conditioning, Izmir, Turkey has been appreciated.

References

Anderson, B.A., Singh, R.P., 2006. Effective heat transfer coefficient measurement during air impingement thawing using an inverse method. International Journal of Refrigeration 29, 281–293.
Baik, O.-D., Marcotte, M., 2002. Modeling the moisture diffusivity in a baking cake. Journal of Food Engineering 56, 27–36.
Broyart, B., Trystram, G., 2002. Modelling heat and mass transfer during the continuous baking of biscuits. Journal of Food Engineering 51, 47–57.
Carnahan, B., Luther, H.A., Wilkes, J.O., 1969. Applied Numerical Methods. Wiley & Sons, Inc., NY. pp. 440–446.
Carson, J.K., Willix, J., North, M.F., 2006. Measurements of heat transfer coefficients within convection ovens. Journal of Food Engineering 72 (3), 293–301.
Carvalho, M., Martins, N., 1993. Mathematical modelling of heat and mass transfer in a forced convection baking oven. AIChE Symposium Series – Heat Transfer 88 (288), 205–211.
Demirkol, E., Erdoğdu, F., Palazoğlu, T.K., 2006. Analysis of mass transfer parameters (changes in mass flux, diffusion coefficient and mass transfer coefficient) during baking of cookies. Journal of Food Engineering 72 (4), 364–371.
Erdoğdu, F., Sarkar, A., Singh, R.P., 2005. Mathematical modeling of air-impingement cooling of finite slab shaped objects and effect of spatial variation of heat transfer coefficient. Journal of Food Engineering 71, 287–294.
Geankoplis, C.J., 2003. Transport processes and separation process principles, fourth ed. Prentice-Hall, Englewood Cliffs, NJ.
Holman, J.P., 1992. Heat Transfer, seventh ed. Mechanical Engineering Series Mc Graw Hill Book Co., Singapore, p. 713p.
Incropera, F.P., Dewitt, D.P., 1996. Introduction to Heat Transfer, third ed. NY, John Wiley & Sons., Inc.. 801p.
Lostie, M., Peczalski, R., Andrieu, J., Laurent, M., 2002. Study of sponge cake batter baking process. II. Modeling and parameter estimation. Journal of Food Engineering 55 (4), 349–357.
Nitin, N., Karwe, M.V., 2001. Heat transfer coefficient for cookie shaped objects in hot air jet impingement oven. Journal of Food Process Engineering 24, 51–69.
Özilgen, M., Heil, J.R., 1994. Mathematical modelling of transient heat and mass transport in a baking process. Journal of Food Processing and Preservation 18, 133–148.
Pan, Z., Singh, R.P., Rumsey, T.R., 2000. Predictive modelling of contact-heating process for cooking a hamburger patty. Journal of Food Engineering 46, 9–19.
Pan, Z., Singh, R.P., 2002. Heating surface temperature and contact-heat transfer coefficient of clam-shell grill. Lebensmittel-Wissenschaft und-Technologie 35 (4), 348–354.
Sablani, S.S., Marcotte, M., Baik, O.-D., Castaigne, F., 1998. Modeling of simultaneous heat and water transport in the baking process. Lebensmittel-Wissenschaft und –Technologie 31, 201–209.
Sakin, M., 2005. Modeling of Cake Baking Process as Simultaneous Heat and Mass Transfer, PhD Thesis, Ege University, Institute of Natural and Applied Sciences, Branch of Food Engineering, Bornova, Izmir.
Sakin, M., Turkkan, M.E., Kaymak-Ertekin, F., 2006. Fırında Pişirme İşleminde Yüzey Isı Aktarım Katsayısının Belirlenmesi (Determination of surface heat transfer coefficient during baking). In: Proceedings of the 9th Food Congress, Bolu, Turkey, in Turkish.
Sakin, M., Kaymak-Ertekin, F., Ilicali, C., 2007a. Modeling the moisture transfer during baking of white cake. Journal of Food Engineering 80, 822–831.
Sakin, M., Kaymak-Ertekin, F., Ilicali, C., 2007b. Simultaneous heat and mass transfer simulation applied to convective oven cup cake baking. Journal of Food Engineering 83, 463–474.
Sato, H., Matsumura, T., Shibukawa, S., 1987. Apparent heat transfer in a forced convection oven and properties of baked food. Journal of Food Science 52 (1), 185–188.
Savoye, I., Trystram, G., Duquenoy, A., Brunet, P., Marchin, F., 1992. Heat and mass transfer dynamic modeling of an indirect biscuit baking tunnel-oven. Part I: Modeling principles. Journal of Food Engineering 16, 173–196.
Singh, R.P., 1982. Thermal diffusivity in food processing. Food Technology 2, 87–91.
Singh, N., Akins, R.G., Erickson, L.E., 1984. Modelling heat and mass transfer during the oven roasting of meat. Journal of Food Process Engineering 7, 205–220.
Standing, C.N., 1974. Individual heat transfer modes in band oven biscuit baking. Journal of Food Science 39, 267–271.
Thorvaldsson, K., Janestad, H., 1999. A model for simultaneous heat, water and vapour diffusion. Journal of Food Engineering 40, 167–172.
Tong, C.H., Lund, D.B., 1990. Effective moisture diffusivity in porous materials as a function of temperature and moisture content. Biotechnology Progress 6, 67–75.
Tszeng, T., Saraf, V., 2003. A study of fin effects in the measurement of temperature using surface-mounted thermocouples. J Heat Transfer, Trans ASME 125 (5), 926–935.
Verboven, P., Datta, A.K., Anh, N.T., Scheerlinck, N., Nicolai, B.M., 2003. Computation of airflow effects on heat and mass transfer in a microwave oven. Journal of Food Engineering 59, 181–190.
Zanoni, B., Peri, C., Pierucci, S., 1993. A study of the bread baking process. I: A phenomenological model. Journal of Food Engineering 19, 389–398.
Zanoni, B., Peri, C., Pierucci, S., 1994. A study of the bread baking process. II: Mathematical modeling. Journal of Food Engineering 23, 321–336.